Catalysis Today 148 (2009) 310–315

Contents lists available at ScienceDirect

Catalysis Today

journal homepage: www.elsevier.com/locate/cattod

$Na_2WO_4/Mn/SiO_2$ catalyst for oxidative dehydrogenation of ethane using CO_2 as oxidant

Jianqiang Zhu, Song Qin, Songtao Ren, Xiaoxi Peng, Dongmei Tong, Changwei Hu *

Key Laboratory of Green Chemistry and Technology, Ministry of Education, College of Chemistry, Sichuan University, Chengdu, Sichuan 610064, China

ARTICLE INFO

Article history:
Available online 13 August 2009

Keywords:
Ethane
CO_2
Ethylene
Synthesis gas
$Na_2WO_4/Co–Mn/SiO_2$

ABSTRACT

Co-promoted $Na_2WO_4/Mn/SiO_2$ catalysts were prepared and used in the reaction of C_2H_6 with CO_2. XRD, XPS techniques were employed to study the structure of the fresh and post-reacted catalysts. It was found that the existence of Co was in favor of the reforming of C_2H_6 to synthesis gas. The Co species were reduced into metal Co, which might act as the active phase for CO production. Over Co-promoted $Na_2WO_4/Mn/SiO_2$ catalysts in the reaction process, the oxidative dehydrogenation and reforming of ethane by CO_2 might be tuned. Under the conditions of $C_2H_6/CO_2 = 1/5$, $F = 60$ ml/min, 750 °C, the catalyst dosage of 0.3 g, products with molar ratio of $C_2H_4/CO/H_2 = 1/1/1$ could be obtained from C_2H_6 and CO_2, and could be used directly into hydroformylation to propanal.

1. Introduction

The catalytic conversions of light alkanes to corresponding alkenes are investigated extensively for its energy-saving character. Ethylene, as an important intermediate, is mainly produced by steam cracking of hydrocarbons. The oxidative dehydrogenation of ethane (ODE) is a promising route for ethylene production. Many researches [1–7] proved that several metal oxides, such as gallium oxide, chromium oxide, vanadium oxide, molybdenum oxide and nickel oxide were effective in the oxidative dehydrogenation of ethane. Carbon dioxide, as a greenhouse gas, is a promising and mild oxidant for the dehydrogenation of ethane. Compared to O_2, CO_2 possesses several advantages, because CO_2 can act as a medium for heat supplying and maintain the catalyst life by removing coke formed on the catalyst surface [8]. Although there are merits in ODE reaction with CO_2, the cost of the separation and the utilization of H_2 and CO generated in the above reaction should be taken into account.

Alternatively, we noticed that the mixture of C_2H_4, H_2 and CO with a molar ratio of $C_2H_4/CO/H_2 = 1/1/1$ can be directly used as feedstock for hydroformylation to propanal. In our previous studies [9], the gas mixture with a molar ratio of $C_2H_4/CO/H_2 = 1/1/1$ was obtained simultaneously in dual catalyst bed system from oxidative coupling of methane (OCM), using $Na_2WO_4/Mn/SiO_2$ and $Co/\gamma\text{-}Al_2O_3$ as the catalysts. However, because of the low methane conversion, the yield of ethylene just reached about 13.0%, which needed to be improved for further industrialization.

On the contrary, in the dehydrogenation of ethane with CO_2, the products consisting of ethylene with relatively high concentrations can be obtained. Synthesis gas, however, is often yielded as the major by-products with lower concentrations. Since the relative molar ratio of synthesis gas is less than that of ethylene in ODE with CO_2 in general, it becomes effective to improve the proportion of synthesis gas in term of enhancing synthesis gas production. Co-based catalysts, for instance, are reactive for partial oxidation of low hydrocarbons to produce synthesis gas. Many studies on the Co-based catalysts were reported in the partial oxidative of methane (POM) and ethane (POE) [10–15]. Nishimoto et al. [16] found that Co-loaded on oxidized diamond catalysts exhibited excellent performance for this reaction without carbon deposition for prolonged experiments.

The $Na_2WO_4/Mn/SiO_2$ catalyst system was first reported by Fang et al. [17,18] for the oxidative coupling of methane in 1992, and then this system has been extensively studied by many research groups [19–24] for its excellent catalytic performance in OCM reaction. In a single-pass operation, 66.9% selectivity at 37.7% CH_4 conversion could be obtained [17]. Up to 80.0% C_2 selectivity at 33.0% CH_4 conversion over this catalyst system had been reported by Palermo et al. [19]. Ji et al. [25] proposed that the surface WO_4 tetrahedron is essential to the oxidative coupling of methane over $Na_2WO_4/Mn/SiO_2$ catalyst.

In this paper, we proposed a new strategy to convert ethane and CO_2 to synthesis gas and ethylene in desired relative molar ratios ($C_2H_4/CO/H_2 = 1/1/1$). $Na_2WO_4/Mn/SiO_2$, one of the effective catalysts in OCM for ethylene production [20–23] is employed as an ODE catalyst. Because Co-based catalysts are reactive for partial oxidation of low hydrocarbons to produce synthesis gas, especially for CO-rich synthesis gas production, we investigated the effect of Co addition on the performance of $Na_2WO_4/Mn/SiO_2$ catalyst in ODE reaction with CO_2 to produce synthesis gas and ethylene simultaneously.

* Corresponding author. Tel.: +86 28 85411105; fax: +86 28 85411105.
E-mail addresses: chwehu@mail.sc.cninfo.net, gchem@scu.edu.cn (C. Hu).

0920-5861/$ – see front matter © 2009 Elsevier B.V. All rights reserved.
doi:10.1016/j.cattod.2009.07.074

2. Experimental

2.1. Catalysts preparation

The Na_2WO_4(5 wt%)/Co(x wt%)–Mn(2 wt%)/SiO_2 catalysts, noted as Co(x), where x donated the percentage of Co in the catalyst, were prepared by incipient wetness impregnation method. The SiO_2 support (20–40 mesh, 317 m^2/g) was impregnated with aqueous solution containing appropriate concentrations of both $Mn(NO_3)_2$ and $Co(NO_3)_2$ for 24 h and dried at 120 °C for 4 h, then calcined at 800 °C for 5 h. The thus-obtained samples were then impregnated with Na_2WO_4 aqueous solution for 24 h and dried at 120 °C for 4 h, and finally calcined at 800 °C for 5 h.

The Na_2WO_4(5 wt%)/SiO_2, Co(12 wt%)/SiO_2 and Mn(2 wt%)/SiO_2 catalysts were prepared by impregnation of SiO_2 support (20–40 mesh, 317 m^2/g) with aqueous solutions containing appropriate concentrations of corresponding precursors for 24 h and dried at 120 °C for 4 h, then calcined at 800 °C for 5 h.

2.2. Catalytic activity test

The catalytic activity test was carried out in a fixed-bed flow micro-quartz-tube reactor under ambient atmospheric pressure. 0.3 g granular catalyst with 20–40 mesh was loaded in the middle of the reactor. The catalyst was heated from room temperature to reaction temperature (750 °C) at the rate of 10 K/min in a flow of Argon (99.99%, 20 ml/min) before the introduction of reactant gases. Then the reactants, C_2H_6 (99.95%) and CO_2 (99.95%) with suitable molar ratio, were co-fed into the reactor without any diluents. The flow rate of reactant gases were controlled by mass flow controllers (D07-11A/ZM made by Beijing Sevenstar Huachuang Electronic Co. Ltd.). At the reactor outlet, a cold trap and a desiccator were employed to remove the water from the effluent stream. Then the effluent after removal of water was analyzed by an on-line gas chromatograph (Agilent 1790 GC) with a plot-C2000 capillary column for separating the products and a TCD to determine the amount of each component. Each data discussed in this paper was obtained after the reaction got its stabilization state in about 10 h, and the deviation of the activity was ±0.2%. The conversions of reactants and the selectivities of products were calculated assuming that the hydrocarbons in the effluent gas (C_2H_4 and CH_4) came from C_2H_6 while CO came from CO_2 and C_2H_6.

2.3. Catalyst characterization

The fresh and post-reacted catalysts were comparatively characterized by XRD and XPS techniques. The X-ray diffraction patterns of the catalysts were obtained with a DX-1000 CSC diffractometer using Cu Ka monochromatic radiation X-ray. The unit was operated at 40 kV and 25 mA over the scattering angle of 2θ from 10° to 70° with a step of 0.06°/min. The XPS measurements of the catalysts were carried out with a XSAM800 spectrometer using Al Ka radiation, and the binding energy was calibrated with XPS signals of C1s at 284.8 eV. The surface compositions of each component were calculated from peak areas using the sensitivity factors, which were provided from the software of the instrument.

3. Results and discussion

3.1. Characterization of the catalysts

3.1.1. XRD results

The fresh and post-reacted catalysts with different Co loadings were characterized by X-ray diffraction and the results were presented in Figs. 1 and 2, respectively. As shown in Fig. 1, α-cristobalite existed in all of the fresh catalysts, and the diffraction intensity decreased with increasing loading of Co promoter. Especially, when the loading of Co was more than 4%, the peak intensity of α-cristobalite decreased drastically. The peaks for Co_2O_3 and Co_3O_4, however, were not observed in the XRD patterns. Instead, the peak assigned to $CoWO_4$ could be detected in Co(2) catalyst, and its intensity increased slightly in Co(4) catalyst. When the loading of Co increased from 8 to 12 wt%, the crystalline of $CoWO_4$ disappeared and the diffraction peaks assigned to $CoSiO_3$ were observed. When the loading of Co increased to 16 wt%, the peaks corresponding to Co_2SiO_4 were observed while those for $CoSiO_3$ could not be detected. The decreasing peak intensity for α-cristobalite accompanied by the formation of metasilicate or silicate species suggested that the existence of Co destruct the crystalline of α-cristobalite in certain extent. The crystalline form of Mn_2O_3 appeared only in Na_2WO_4/Mn/SiO_2 and Co(0.5) catalyst. These data indicated that complex interactions between the components existed depending on the amount of Co added.

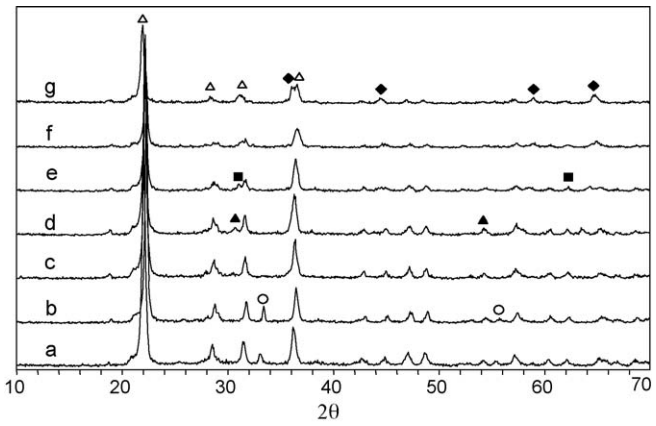

Fig. 1. The XRD profiles of the fresh catalysts. (a) Na_2WO_4/Mn/SiO_2; (b) Co(0.5); (c) Co(2); (d) Co(4); (e) Co(8); (f) Co(12); (g) Co(16). Symbols: α-cristobalite (△); $CoWO_4$ (▲); $CoSiO_3$ (■); Mn_2O_3 (○); Co_2SiO_4 (◆).

As compared to the fresh catalysts, additional peaks assigned to quartz phase were observed on all of the post-reacted catalysts. The existence of crystalline of quartz illustrated that a part of α-cristobalite was transformed into quartz, which is in accordance with the results observed in OCM reaction [26]. After the reaction of ODE with CO_2, the peaks assigned to Mn_2O_3 and/or MnO_2 disappeared. $NaCoO_2$ was detected only in Co(2) catalyst. When the loading of Co exceeded 2 wt%, crystalline metal Co started to appear and the peak intensity increased with further increase of Co

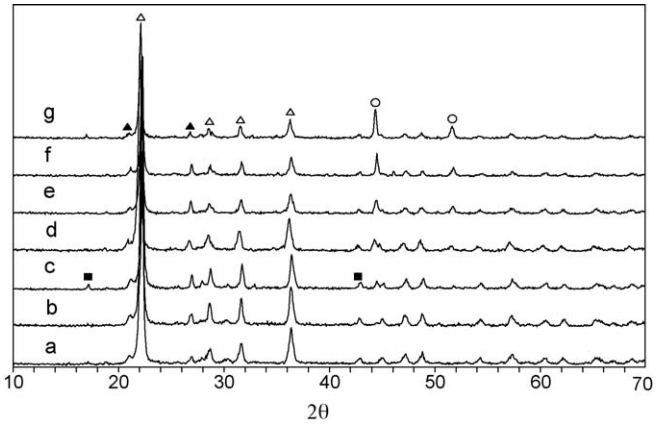

Fig. 2. The XRD profiles of the post-reacted catalysts. (a) Na_2WO_4/Mn/SiO_2; (b) Co(0.5); (c) Co(2); (d) Co(4); (e) Co(8); (f) Co(12); (g) Co(16). Symbols: $NaCoO_2$ (■); α-cristobalite (△); quartz (▲); Co (○).

Table 1
The surface compositions (at%) of the components of the fresh catalysts.

Catalyst	Na(1s) (at%)	W(4f) (at%)	Co(2p) (at%)	Mn(2p) (at%)	Si(2p) (at%)	O(1s) (at%)	Na/W
$Na_2WO_4/Mn/SiO_2$	7.21	4.10	0	1.50	23.85	63.34	1.76
$Na_2WO_4/Co(0.5)–Mn/SiO_2$	5.93	1.24	1.64	1.11	25.36	64.72	4.78
$Na_2WO_4/Co(2)–Mn/SiO_2$	5.95	1.47	1.96	2.12	24.92	63.58	4.05
$Na_2WO_4/Co(4)–Mn/SiO_2$	5.03	1.41	1.99	1.75	25.48	64.35	3.57
$Na_2WO_4/Co(8)–Mn/SiO_2$	5.32	0.95	2.51	2.11	24.77	64.33	5.60
$Na_2WO_4/Co(12)–Mn/SiO_2$	5.78	1.06	4.61	2.12	23.41	63.02	5.45
$Na_2WO_4/Co(16)–Mn/SiO_2$	5.10	0.93	4.66	1.47	25.44	62.40	5.48

Table 2
The surface compositions (at%) of the components of the post-reacted catalysts.

Catalyst	Na(1s) (at%)	W(4f) (at%)	Co(2p) (at%)	Mn(2p) (at%)	Si(2p) (at%)	O(1s) (at%)	Na/W
$Na_2WO_4/Mn/SiO_2$	6.86	1.84	0	2.65	23.70	64.95	3.73
$Na_2WO_4/Co(0.5)–Mn/SiO_2$	6.10	2.00	0	2.33	23.72	65.85	3.05
$Na_2WO_4/Co(2)–Mn/SiO_2$	6.38	1.98	1.60	2.25	24.42	63.37	3.22
$Na_2WO_4/Co(4)–Mn/SiO_2$	6.13	2.40	4.03	1.71	21.68	64.05	2.55
$Na_2WO_4/Co(8)–Mn/SiO_2$	5.74	2.28	4.08	2.11	22.59	63.21	2.52
$Na_2WO_4/Co(12)–Mn/SiO_2$	6.09	2.07	5.46	1.89	21.76	62.73	2.94
$Na_2WO_4/Co(16)–Mn/SiO_2$	6.38	2.36	6.04	2.43	20.47	62.33	2.70

loading. Especially, when the loading exceeded 4 wt%, the peak intensity corresponding to metal Co increased obviously. The intensity of α-cristobalite phase decreased with increasing loading of Co, but it was still greater than that of the corresponding one of fresh catalyst. The above results indicated that the Co species were reduced and a part of α-cristobalite crystalline should be recovered after the reaction.

3.1.2. XPS results

The surface compositions of fresh Co-promoted $Na_2WO_4(5)/Mn(2)/SiO_2$ catalysts were measured by XPS technique. The results were listed in Table 1.

For all the fresh catalysts, there was little difference in binding energies for all the elements, which illustrated that the oxidation states of the surface species were not altered with the addition of Co promoter. A part of the surface sodium might be presented in a form other than Na_2WO_4, as the surface Na/W atomic ratio was higher than 2. This is in accordance with the results reported in our previous investigation [23]. As shown in Table 1, with the addition of Co, the surface concentrations of Na and W decreased obviously. This implied that the addition of Co was inhibitory for the enriching of Na and W on the catalyst surface.

As shown in Table 2, the surface concentration of Na and W became larger on the Co-promoted catalysts after the reaction, and the atomic ratio of Na/W was still more than 2. It should be noted that, when the amount of loading was less than 2 wt%, the concentration of Co species was decreased as compared to that of the fresh catalyst. Especially, we cannot detect surface Co species on Co(0.5). On the contrary, when the amount of loading exceeded 4 wt%, the surface concentration of Co increased. These results suggested that after the reaction, Co species on the surface could disperse well when the loading amount was less than 2 wt% and aggregate when the loading amount was more than 4 wt%, which is in accordance with the XRD results mentioned above.

3.2. Catalytic performance

3.2.1. Effects of Co loading

Under the conditions of $C_2H_6/CO_2 = 1/5$, $F = 60$ ml/min,750 °C, the catalyst dosage of 0.3 g, the catalytic behavior of $Na_2WO_4(5)/Mn(2)/SiO_2$ in ODE with CO_2 was investigated firstly. As shown in Table 3, over the $Na_2WO_4(5)/Mn(2)/SiO_2$ catalyst without Co addition, the conversions of C_2H_6 and CO_2 were 50.5 and 9.0%, respectively, and the selectivity of C_2H_4 was 94.2%. For this system, the molar ratio of $C_2H_4/CO/H_2$ obtained was 1/0.49/0.92 with the C_2H_4 yield of 47.6%. However, the concentration of CO was relatively low.

On the other hand, when $Na_2WO_4/Mn/SiO_2$ catalyst was modified with Co, the conversions of C_2H_6 and CO_2 exceeded 55.6 and 10.0%, respectively, indicating that the addition of Co moderately improved the catalytic activities of $Na_2WO_4/Mn/SiO_2$. Under the same reaction conditions, especially over Co(2) catalyst, the conversion of C_2H_6 reached the maximum value of 60.3%, and over Co(8) catalyst, the conversion of CO_2 reached the maximum value of 15.0%. The selectivity of C_2H_4 kept almost constant around 93% over the majority of catalysts, however, it dropped to the minimum value of 84.7% over Co(16) catalyst, which might be due to the fact that the excessive Co promoter inhibited the ODE reaction partially and favored the reforming of C_2H_6 by CO_2. The molar ratio of CO in products increased almost monotonically with the increase of Co loading firstly, and reached about 1 over Co(4). When the amount of Co loading exceeded 4 wt%, the molar ratio of $C_2H_4/CO/H_2$ changed slightly, and the desired molar ratio can be obtained over Co(4), Co(8), Co(12) and Co(16) catalysts. The molar ratio of H_2 was fluctuant over the range of 0.91–1.03. Under the condition of $C_2H_6/CO_2 = 1/5$, $F = 60$ ml/min, 750 °C, the catalyst dosage of 0.3 g, the optimum value of $C_2H_4/CO/H_2 = 1/1/1$ over Co(12) catalyst can be obtained with the C_2H_4 yield of 51.6%, which was fairly suitable for directly use in hydroformylation to propanal.

To evaluate the exact effects of Co species in this reaction system, the catalytic performances of sole component supported

Table 3
The influence of Co loading on the catalytic performance.

Catalyst	Conv. (%)		Sele. (%)	Yield (%)	$C_2H_4/CO/H_2$
	C_2H_6	CO_2	C_2H_4	C_2H_4	
$Na_2WO_4/Mn/SiO_2$	50.5	9.0	94.2	47.6	1/0.49/0.92
$Na_2WO_4/Co(0.5)–Mn/SiO_2$	56.0	10.0	93.6	52.3	1/0.56/0.95
$Na_2WO_4/Co(2)–Mn/SiO_2$	60.3	12.6	90.7	54.7	1/0.76/0.96
$Na_2WO_4/Co(4)–Mn/SiO_2$	56.2	14.7	93.5	52.5	1/0.93/1.03
$Na_2WO_4/Co(8)–Mn/SiO_2$	55.8	15.0	92.8	51.8	1//0.97/0.91
$Na_2WO_4/Co(12)–Mn/SiO_2$	55.6	14.7	92.9	51.6	1/1.00/1.00
$Na_2WO_4/Co(16)–Mn/SiO_2$	56.6	13.8	84.7	48.0	1/1.03/0.98

Table 4
A comparison of catalytic performances of different catalysts.

Catalyst	Conv. (%)		Sele. (%)	Yield (%)	$C_2H_4/CO/H_2$	C balance (%)
	C_2H_6	CO_2	C_2H_4	C_2H_4		
Empty tube (C_2H_6/Ar)	65.6	–	84.2	55.2	1/0/1.02	85.5
Empty tube (C_2H_6/CO_2)	57.5	6.0	98.2	56.7	1/0/1.00	96.2
Mn(2)/SiO_2	52.9	10.0	99.5	53.4	1/0.42/1.00	97.3
Na_2WO_4(5)/SiO_2	58.3	10.1	98.4	57.4	1/0.49/0.99	96.8
Co(12) /SiO_2	69.2	32.5	56.6	39.2	1/3.92/1.67	91.3
Na_2WO_4/Mn/SiO_2	50.5	9.0	94.2	47.6	1/0.49/0.92	95.4
Na_2WO_4/Co(12)–Mn/SiO_2	55.6	14.7	92.9	51.6	1/1.00/1.00	96.3

on SiO_2 were also comparably investigated, and the results were presented in Table 4. The conversion of C_2H_6 (57.5%) and the selectivity of C_2H_4 (98.2%) in the blank experiment suggested that both the thermal cracking of C_2H_6 and the oxidative dehydrogenation by CO_2 may occur readily in the absence of catalyst. When Ar was substituted to CO_2 in the blank experiment, the conversion of C_2H_6 increased to 65.6%, but the selectivity of C_2H_4 (84.2%) as well as the carbon balance of 85.5% suggested that the thermal cracking of C_2H_6 mainly proceeded with coke formation in the absence of CO_2. On the other hand, the Mn(2)/SiO_2, Na_2WO_4(5)/SiO_2 and Na_2WO_4/Mn/SiO_2 catalysts exhibited a moderate activity for the reforming of C_2H_6 by increasing the conversion of CO_2. Over Co(12)/SiO_2 catalyst, as compared to other catalysts, the conversions of C_2H_6 and CO_2 were much higher, which reached 69.2 and 32.5%, respectively, while the selectivity and corresponding yield of C_2H_4 decreased to 56.6 and 39.2%, respectively. Therefore, the molar ratios of CO and H_2 in products were higher than that of ethylene. It was obvious that the Co species was effective for the conversions of C_2H_6 and CO_2.

3.2.2. The optimization of reaction conditions

As shown in Table 3, it was found that the conversion of CO_2 was relatively low. It might be attributed to the fact that CO_2 was much more excessive than C_2H_6 under the above reaction condition (C_2H_6/CO_2 = 1/5). In order to improve the conversion of CO_2 to the target products, the influence of C_2H_6/CO_2 on the reaction was also tested over Co(12) catalyst by keeping the total flow rate and the reaction temperature constant. The catalytic performance got its stable situation in about 3 h, and the results obtained after 10 h were listed in Table 5.

As shown in Table 5, the conversion of C_2H_6 increased from 55.6% (C_2H_6/CO_2 = 1/5) and reached the maximum of 62.8% (C_2H_6/CO_2 = 1/1) in the range of 1/5 to 1/1, and then decreased with further increase of C_2H_6/CO_2. With the increase of C_2H_6/CO_2, the conversion of CO_2 increased continuously from 14.7 to 45.1%, whereas the selectivity and the corresponding yield of C_2H_4 decreased sharply from 92.9 and 51.6% to 45.4 and 25.2%, respectively. It should be noted that the carbon balance decreased gradually with increasing C_2H_6/CO_2 ratio, which indicated increasing carbon deposition. In another control experiment with a molar ratio of C_2H_6/CO_2 = 5/1, the deposited carbon could block the reactor within about 3 h, which confirmed the above deduction. It is shown that sufficient amount of CO_2 must be provided to the reaction system in order to remove the coke formed from ethane cracking.

The influence of total flow rate was studied over Co(12) catalyst by keeping the C_2H_6/CO_2 = 1/5 and the reaction temperature constant. As shown in Table 6, it was found that the conversions of C_2H_6 and CO_2 decreased with the increase of total flow rate in the entire range, from 65.3 and 19.1% to 41.2 and 10.5%, respectively. This might be due to that the increase of flow rate resulted in the decline of the contact time on the catalyst surface. However, the selectivity of C_2H_4 increased from 83.6 to 98.3%, and the carbon balance exceeded 94.0% and increased slightly. This implies that the thermal cracking of ethane is a kinetically controlled process, and short contact time favors the selectivity of ethylene and inhibits carbon deposition. However the ODE and/or reforming of ethane by CO_2 need sufficient contact time. The deposited carbon could be neglected for its little amount. Therefore, the net result was the decline of CO production with increasing flow rate.

3.2.3. The role of CO_2 in the reaction system

At the reaction temperature of 750 °C, the pyrolysis of C_2H_6 to carbon formation was inevitable. As mentioned above, in the present system, the thermal cracking of C_2H_6 and the reforming of C_2H_6 by CO_2 occurred simultaneously. Many researchers [2,8] reported that CO_2 can remove coke formed from the thermal cracking on the catalyst surface. A comparison of the yield of CO and the conversion of C_2H_6 showed that the formation of CO not only originated from CO_2 but also from C_2H_6. Decreasing the proportion of CO_2 in the feed resulted in not only the decrease of the amount of the carbon deposited being oxidized to CO by CO_2 but also the decrease of reforming of C_2H_6 by CO_2. As mentioned above, it is clearly seen from the comparison of the blank experiments with the catalyzed ones that the increase of carbon balance and CO yield in the presence of CO_2 suggested the steadily occurrence of reforming of C_2H_6 by CO_2.

3.2.4. Effects of Co phases on the reaction

Over Na_2WO_4/Co(12)–Mn/SiO_2 catalyst, the yield of C_2H_4 varied from 68.0% at the beginning to 54.0% in about 3 h and then kept almost the constant value of 52.0%. The conversion of CO_2

Table 5
The influence of C_2H_6/CO_2 on the catalytic performance.

C_2H_6/CO_2	Conv. (%)		Sele. (%)	Yield (%)	$C_2H_4/CO/H_2$	C balance (%)
	C_2H_6	CO_2	C_2H_4	C_2H_4		
1/5	55.6	14.7	92.9	51.6	1/1.00/1.00	96.3
1/3	61.5	22.5	77.1	47.4	1/1.14/1.06	92.5
1/1	62.8	43.8	53.4	33.5	1/1.51/1.32	84.6
3/1	55.5	45.1	45.4	25.2	1/1.06/1.23	80.2

Table 6
The influence of total flow rate on the catalytic performance.

F (ml/min)	Conv. (%)		Sele. (%)	Yield (%)	$C_2H_4/CO/H_2$	C balance (%)
	C_2H_6	CO_2	C_2H_4	C_2H_4		
30	65.3	19.1	83.6	54.6	1/1.24/1.23	94.1
45	60.3	15.7	89.5	54.0	1/1.13/1.02	95.0
60	55.6	14.7	92.9	51.6	1/1.00/1.00	96.3
75	47.4	11.5	96.5	45.8	1/0.72/0.88	96.6
90	41.2	10.5	98.3	40.5	1/0.70/0.93	97.4

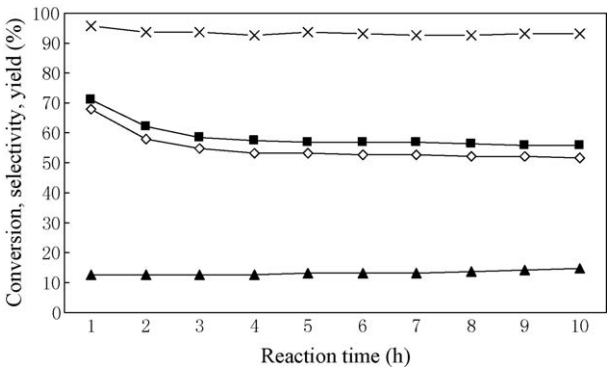

Fig. 3. The catalytic activity and stability of Co(12) versus reaction time. (■) The conversion of C_2H_6, (▲) the conversion of CO_2, (×) the selectivity of C_2H_4, (◇) the yield of C_2H_4.

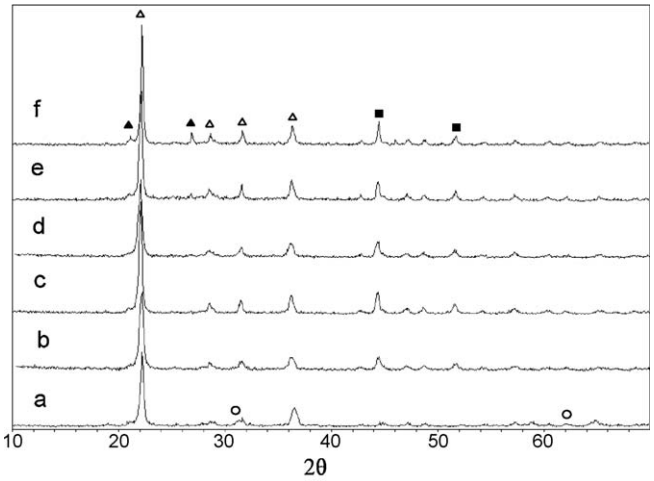

Fig. 5. The XRD profiles of Co(12) catalyst with different reaction time. (a) Fresh catalyst; (b) 2 h; (c) 4 h; (d) 6 h; (e) 8 h; (f) 10 h. Symbols: α-cristobalite (△); quartz (▲); Co (■); $CoSiO_3$ (○).

increased from 12.5 to 14.7%. The catalytic activity and stability of Na_2WO_4/Co(12)–Mn/SiO_2 catalyst along with the reaction time were presented in Fig. 3, and the distribution of products versus reaction time was plotted in Fig. 4. To identity the structural evolution of Na_2WO_4/Co(12)–Mn/SiO_2 catalyst along with the reaction, the fresh and post-reacted catalysts with different reaction time were characterized by XRD and the results were comparably presented in Fig. 5.

As shown in Fig. 3, the conversion of C_2H_6 decreased sharply within 2 h, and then decreased slightly along with the proceeding of reaction. The conversion of CO_2 exhibited a slight increase. In contrast, the selectivity of C_2H_4 maintained at a constant value of 93.0% after 2 h, and the corresponding yield of C_2H_4 decreased slightly. On the other hand, as shown in Fig. 4, the ratio of H_2/C_2H_4 was slightly fluctuant around 1, further suggesting the dehydrogenation of C_2H_6 proceeded steadily. However, the ratio of CO/C_2H_4 increased from 0.6 at the beginning and reached 1 in about 7 h.

The XRD profiles of Na_2WO_4/Co(12)–Mn/SiO_2 catalyst showed the appearance of peaks assigned to Co within 2 h. The intensity of these peaks increased at the reaction time of 4 h and varied slightly with the proceeding of reaction. Therefore, it was reasonable to deduce that Co species might be reduced by CO and/or H_2 generated from the reaction. After 4 h of the reaction, the reduction of Co completed. Correspondingly, the molar ration of CO/C_2H_4 increased to about 0.8, suggesting that Co metal was responsible for the steady production of CO. It was also found that the new peaks assigned to quartz started to appear after the reaction time of 8 h, and became more obvious at the reaction time of 10 h. While the intensity of α-cristobalite phase increased with the increase of reaction time, it might illustrate that a part of α-cristobalite crystalline should be recovered gradually along with the reaction proceeded.

By combining the XRD results and catalytic performance, we hypothesized the potential effects of Co promoter as follows: (1) Co catalyst was effective in the reforming of C_2H_6 by CO_2, and especially facilitated the production of CO. This is in accordance with the results of Iwasaki et al. [27]. (2) The addition of Co could improve the catalytic activity even with low loading. In the present work, the conversion of C_2H_6 and CO_2 increased after the addition of Co promoter. (3) The addition of Co destructed the crystalline of α-cristobalite of the catalysts. During the reaction, the Co promoter could facilitate the migration of Na and W from the bulk to the catalyst surface.

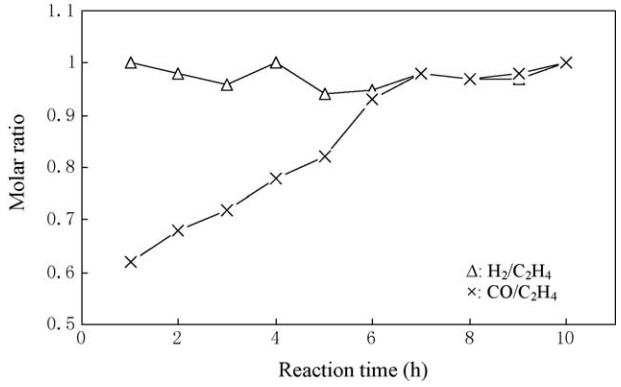

Fig. 4. The evolution of molar ratios of H_2/C_2H_4 and CO/C_2H_4 along the reaction time.

4. Conclusions

Over Co-promoted Na_2WO_4/Mn/SiO_2 catalyst, the synthesis gas and ethylene with the molar ratio of C_2H_4/CO/H_2 = 1/1/1 can be obtained under the optimal conditions: C_2H_6/CO_2 = 1/5, F = 60 ml/min, 750 °C, the catalyst dosage of 0.3 g, and the product gases can be used directly into hydroformylation to propanal.

Co exhibited different affinities to combine WO_4 at low loading and SiO_2 at high loading. During the reaction, the Co species were reduced and a part of α-cristobalite crystalline should be recovered. When the loading of Co exceeded 2 wt%, crystalline metal Co started to appear and the metal particles become larger with further increase of Co loading. The addition of Co was inhibitory for the enriching of Na and W on the catalyst surface.

CO_2 can remove the coke formed on the catalyst surface and facilitate the reforming of ethane for CO production. Co promoter improved the catalytic performance moderately by enhancing the reforming of ethane with CO_2. Co promoter could also destruct the crystalline of α-cristobalite. The Co species were reduced into metal Co during the reaction, which might act as the active phase for CO production.

Acknowledgements

The authors are grateful for financial support from the NNSFC (No. 20243006), the Special Research Foundation of Doctoral Education of China (No. 2000061028), and the characterization of the catalysts from Analytical and Testing Center of Sichuan University.

References

[1] Z.H. Shen, J. Liu, H.L. Xu, Y.H. Yue, W.M. Hua, W. Shen, Appl. Catal. A: Gen. 356 (2009) 148.
[2] G. Karamullaoglu, T. Dogu, Ind. Eng. Chem. Res. 46 (2007) 7079.
[3] T.V.M. Rao, Y. Yang, A. Sayari, J. Mol. Catal. A: Chem. 301 (2009) 152.
[4] K.-I. Nakamura, T. Miyake, T. Konishi, T. Suzuki, J. Mol. Catal. A: Chem. 260 (2006) 144.
[5] L. Lisi, G. Ruoppolo, M.P. Casaletto, P. Galli, M.A. Massucci, P. Patrono, F. Pinzari, J. Mol. Catal. A: Chem. 232 (2005) 127.
[6] N. Haddad, E. Bordes-Richard, A. Barama, Catal. Today 142 (2009) 215.
[7] N. Haddad, E. Bordes-Richard, L. Hilaire, A. Barama, Catal. Today 126 (2007) 256.
[8] X.J. Shi, S.F. Ji, K. Wang, C.Y. Li, Energy Fuels 22 (2008) 3631.
[9] C.W. Hu, J.J. Wu, H.L. Zhang, S. Qin, AIChE J. 53 (2007) 2925.
[10] X.X. Gao, C.J. Huang, N.W. Zhang, J.H. Li, W.Z. Weng, H.L. Wan, Catal. Today 131 (2008) 211.
[11] H.Y. Wang, E. Ruckenstein, J. Catal. 199 (2001) 309.
[12] S. Naito, H. Tanaka, S. Kado, T. Miyao, S. Naito, K. Okumura, K. Kunimori, K. Tomishige, J. Catal. 259 (2008) 138.
[13] H.H. Wang, Y. Cong, W.S. Yang, J. Membr. Sci. 209 (2002) 143.
[14] S.S.A. Syed-Hassan, W.J. Lee, C.Z. Li, J. Membr. Sci. 147 (2009) 307.
[15] S.L. Liu, G.X. Xiong, S.S. Sheng, W.S. Yang, Appl. Catal. A: Gen. 198 (2000) 261.
[16] H. Nishimoto, K. Nakagawa, N. Ikenaga, M. Nishitani-Gamo, T. Ando, T. Suzuki, Appl. Catal. A: Gen. 264 (2004) 65.
[17] X.P. Fang, S.B. Li, J.Z. Lin, J.F. Gu, D.X. Yang, J. Mol. Catal. (China) 6 (1992) 255.
[18] X.P. Fang, S.B. Li, J.Z. Lin, Y.L. Chu, J. Mol. Catal. (China) 6 (1992) 427.
[19] A. Palermo, J.P.H. Vazquez, A.F. Lee, M.S. Tikhov, R.M. Lambert, J. Catal. 177 (1998) 259.
[20] J.X. Wang, L.J. Chou, B. Zhang, H.L. Song, J. Zhao, J. Yang, S.B. Li, J. Mol. Catal. A: Chem. 245 (2006) 272.
[21] S. Pak, J.H. Lunsford, Appl. Catal. A: Gen. 168 (1998) 131.
[22] S. Pak, P. Qiu, J.H. Lunsford, J. Catal. 179 (1998) 222.
[23] J.J. Wu, H.L. Zhang, S. Qin, C.W. Hu, Appl. Catal. A: Gen. 323 (2007) 126.
[24] A. Malekzadeh, A. Khodadadi, M. Abedini, M. Amini, A. Bahramian, A.K. Dalai, Catal. Commun. 2 (2001) 241.
[25] S.F. Ji, T.C. Xiao, S.B. Li, L.J. Chou, B. Zhang, C.Z. Xu, R.L. Hou, A.P.E. York, M.L.H. Green, J. Catal. 220 (2003) 47.
[26] Y.T. Chua, A.R. Mohamed, S. Bhatia, Appl. Catal. A: Gen. 343 (2008) 142.
[27] N. Iwasaki, T. Miyake, E. Yagasaki, T. Suzuki, Catal. Today 111 (2006) 391.